

Probing dense matter in neutron stars with axial w-modes

Debarati Chatterjee and Debades Bandyopadhyay

Theory Division and Centre for Astroparticle Physics,

Saha Institute of Nuclear Physics, 1/AF Bidhannagar, Kolkata-700064, India

Abstract

We study the problem of extracting information about composition and equation of state of dense matter in neutron star interior using axial w-modes. We determine complex frequencies of axial w-modes for a set of equations of state involving hyperons as well as Bose-Einstein condensates of antikaons adopting the continued fraction method. Hyperons and antikaon condensates result in softer equations of state leading to higher frequencies of first axial w-modes than that of nuclear matter case, whereas the opposite happens in case of damping times. The presence of condensates may lead to the appearance of a new stable branch of superdense stars beyond the neutron star branch called the third family. The existence of same mass compact stars in both branches are known as neutron star twins. Further investigation of twins reveal that first axial w-mode frequencies of superdense stars in the third family are higher than those of the corresponding twins in the neutron star branch.

PACS numbers: 97.60.Jd, 26.60.-c, 04.40.Dg

arXiv:0904.1949v1 [astro-ph.HE] 13 Apr 2009

I. INTRODUCTION

Shortly after the discovery of pulsars, the study of dense matter in the core of neutron stars gained momentum [1]. With the advent of satellite based observatories such as Einstein, ROSAT, Hubble space telescope XMM-Newton, and Chandra x-ray observatory, the study of neutron stars has entered into a new era. Observations using these facilities as well as other facilities are pouring in very exciting data on neutron stars. It is now possible to estimate masses, radii, moment of inertia and surface temperatures of neutron stars from the observations. Those findings, in turn, may shed light on the gross properties of cold dense matter far off from normal nuclear matter density in neutron star interior. Such a cold dense matter in the core of a neutron star, so far, has not been produced in laboratories on the earth. Therefore neutron stars are very useful laboratories for the study of highly dense matter in its core.

On the other hand, there is a growing interplay between the physics of dense matter in relativistic heavy ion collisions and that of neutron stars. Though the Quantum Chromodynamics predicts a very rich phase structure of dense matter, we can only probe a small region of it in the laboratories. The study of dense matter in heavy ion collisions reveals many new and interesting results such as the modifications of hadron properties in dense medium, the properties of strange matter including hyperons and (anti)kaons, the strength of attractive antikaon-nucleon interaction and the formation of quark-gluon plasma. These empirical informations from heavy ion collisions may be useful in understanding dense matter in neutron star interior. Heavy ion experiments in the upcoming Facility for Antiproton and Ion Research (FAIR) at GSI, Germany would produce dense matter with baryon density a few times normal nuclear matter density and temperature a few tens of MeV and provide us important information about dense matter.

Gravitational wave astrophysics opens a new window to probe the neutron star interior [2]. Neutron stars are accompanied by strong gravitational field. Non-radial oscillations of neutron stars generate gravitational waves. Such a situation may arise in neutron star glitch, merger of compact stars, a phase transition in the core and gravitational collapse of a massive star. Some large interferometric gravitational wave detectors such as LIGO in USA, VIRGO in Italy and GEO600 in Germany are now operational. A neutron star has a large number of families of pulsation modes [3, 4]. Those modes are classified according to restoring

forces acting on a perturbed fluid element. Important modes among them are fundamental f-mode associated with global oscillations of the fluid, g-mode due to buoyancy and p-mode due to pressure gradient. General relativity also predicts w-modes which are space-time modes. Unlike other pulsation modes of neutron stars, w-modes do not have counterparts in Newtonian gravity. Equations governing perturbation of a static and non-rotating neutron star are decomposed into two sets depending on how perturbations transform under parity. Polar perturbation corresponds to even parity $(-1)^l$ and axial perturbation relates to odd parity $(-1)^{l+1}$. Various groups [5, 6, 7, 8, 9] investigated w-modes in great details and found interesting varieties of axial w-modes [7, 8]. It is to be noted that w-modes have higher frequencies than those of f , g and p modes.

In general relativity, oscillations of neutron stars are damped by gravitational radiation. Consequently, the corresponding oscillatory modes are quasi-normal modes and their frequencies are complex. Once gravitational waves from a neutron star are detected, the spectral analysis of the detected signal would tell us the frequency and damping time of the quasi-normal mode responsible for gravitational waves. Now the question is how we determine the mass, radius and properties of dense matter from the frequency and damping time of the mode. This is achieved by solving the "inverse problem" [3, 10, 11, 12]. To solve this problem, we have to compute frequencies and damping times of modes that could generate strong gravitational waves using different compositions and equations of state and compare them with those obtained from observations. This way we could probe the neutron star interior.

Various novel phases of matter might appear in neutron star interior because of large baryon and lepton chemical potentials there. Glendenning [1] predicted the presence of hyperons in neutron stars. Kaplan and Nelson discussed Bose-Einstein condensation of K^- mesons in neutron star matter due to strongly attractive antikaon-nucleon interaction [13]. The formation of quark matter is another possibility in neutron star core [14]. In this paper, we are motivated to investigate the role of hyperons and antikaon condensation on frequencies of quasi-normal modes of neutron stars. In particular, we would investigate how the strength of antikaon optical potential in nuclear matter which is crucial for antikaon condensation in neutron stars, affects axial w-modes. In this connection, we want to calculate the frequency and damping time of axial w-mode of a neutron star including Bose-Einstein condensate of negatively charged kaons for a set of values of antikaon optical potential depth. Further we

investigate the role of hyperons on frequency and damping time of axial w-modes.

This paper is organised in the following way. The formalism is discussed in section II. Results are explained in section III. Section IV provides summary and conclusions.

II. FORMALISM

Chandrasekhar and Ferrari showed how the problem non-radial oscillations of a compact star could be reduced to the scattering of incident gravitational wave by the static space-time of spherically symmetric star [5, 6]. Here we are interested in axial w-modes of neutron stars. The axial perturbation of the compact star is described by the metric [5, 6, 9]

$$ds^2 = e^{2\nu}(dt)^2 - e^{2\psi}(d\phi - q_2 dr - q_3 d\theta - \omega dt)^2 - e^{2\mu_2}(dr)^2 - e^{2\mu_3}(d\theta)^2, \quad (1)$$

where metric functions ν , ψ , μ_2 and μ_3 retain their unperturbed values and ω , q_2 and q_3 give rise to the perturbations. The radial evolution of equations for axial perturbations is described by the following by the Schrödinger like equation with a potential barrier $V(r)$

$$\left(\frac{d^2}{dr_*^2} + \omega^2 - V(r) \right) Z_l = 0, \quad (2)$$

$$V(r) = \frac{e^{2\nu}}{r^3} (l(l+1)r + r^3[\epsilon(r) - P(r)] - 6M(r)), \quad (3)$$

$$\frac{d\nu}{dr} = -\frac{1}{(\epsilon(r) + P(r))} \frac{dP}{dr}, \quad (4)$$

where the tortoise coordinate is $r_* = \int_0^r e^{-\nu+\mu_2} dr$, $M(r)$ is the mass enclosed in a radius r , ω is the complex frequency of the mode and ϵ and P are energy density and pressure respectively. Both energy and pressure outside the star become zero and the Eq. (2) reduces to the Regge-Wheeler equation with

$$V(r) = \left(1 - \frac{2M}{r} \right) \left(\frac{l(l+1)}{r^2} - \frac{6M}{r^3} \right), \quad (5)$$

and $r^* = r + 2M \ln(r - 2M)$. We determine frequencies of quasi-normal modes by solving Eq. (2) with appropriate $V(r)$ inside and outside the neutron star and boundary conditions such that the solution is regular at the center, continuous at the surface and behaves as a purely outgoing wave at infinity.

Now we focus on the construction of equation of state (EoS) (pressure versus energy density) within relativistic field theoretical models. In this paper, we consider EoS with

different compositions and values of incompressibility of nuclear matter. Firstly we discuss the EoS including neutrons (n), protons (p), hyperons ($H=\Lambda, \Sigma^+, \Sigma^-, \Sigma^0, \Xi^-, \Xi^0$) and electrons (e) and muons(μ). The baryon-baryon interaction is mediated by the exchange of σ , ω , ρ mesons and for hyperon-hyperon interaction, two additional mesons - scalar meson $f_0(975)$ (denoted hereafter as σ^*) and vector meson $\phi(1020)$ [15] are incorporated. Therefore the Lagrangian density for baryons in the charge neutral and β -equilibrated hadronic phase is given by

$$\begin{aligned} \mathcal{L}_B = & \sum_B \bar{\psi}_B (i\gamma_\mu \partial^\mu - m_B + g_{\sigma B} \sigma - g_{\omega B} \gamma_\mu \omega^\mu - g_{\rho B} \gamma_\mu \mathbf{t}_B \cdot \boldsymbol{\rho}^\mu) \psi_B \\ & + \frac{1}{2} (\partial_\mu \sigma \partial^\mu \sigma - m_\sigma^2 \sigma^2) - U(\sigma) \\ & - \frac{1}{4} \omega_{\mu\nu} \omega^{\mu\nu} + \frac{1}{2} m_\omega^2 \omega_\mu \omega^\mu - \frac{1}{4} \boldsymbol{\rho}_{\mu\nu} \cdot \boldsymbol{\rho}^{\mu\nu} + \frac{1}{2} m_\rho^2 \boldsymbol{\rho}_\mu \cdot \boldsymbol{\rho}^\mu + \mathcal{L}_{YY} . \end{aligned} \quad (6)$$

The isospin multiplets for baryons $B = N, \Lambda, \Sigma$ and Ξ are represented by the Dirac spinor Ψ_B with vacuum baryon mass m_B and isospin operator \mathbf{t}_B and $\omega_{\mu\nu}$ and $\rho_{\mu\nu}$ are field strength tensors. The scalar self-interaction term [16] is

$$U(\sigma) = \frac{1}{3} g_2 \sigma^3 + \frac{1}{4} g_3 \sigma^4 . \quad (7)$$

The Lagrangian density for hyperon-hyperon interaction (\mathcal{L}_{YY}) is given by

$$\begin{aligned} \mathcal{L}_{YY} = & \sum_B \bar{\Psi}_B (g_{\sigma^* B} \sigma^* - g_{\phi B} \gamma_\mu \phi^\mu) \Psi_B \\ & + \frac{1}{2} (\partial_\mu \sigma^* \partial^\mu \sigma^* - m_{\sigma^*}^2 \sigma^{*2}) - \frac{1}{4} \phi_{\mu\nu} \phi^{\mu\nu} + \frac{1}{2} m_\phi^2 \phi_\mu \phi^\mu . \end{aligned} \quad (8)$$

As nucleons do not couple with strange mesons, $g_{\sigma^* N} = g_{\phi N} = 0$.

Next we discuss equations of state undergoing first order phase transitions from nuclear to K^- condensed matter denoted by $\text{np}K^-$ and hyperon matter to \bar{K} (K^-, \bar{K}^0) condensed matter denoted by $\text{npH}\bar{K}$. Here we have pure hadronic phase described by Eq. (6) and antikaon condensed phases and the mixed phase of two pure phases. The constituents of β -equilibrated matter in both phases are neutrons, protons, hyperons, electrons and muons. Baryons are embedded in the condensate in the condensed phase. We describe the interaction of (anti)kaons in a relativistic field theoretical model. The Lagrangian density for (anti)kaons in the minimal coupling scheme is [17, 18, 19, 20, 21],

$$\mathcal{L}_K = D_\mu^* \bar{K} D^\mu K - m_K^{*2} \bar{K} K , \quad (9)$$

where the covariant derivative is $D_\mu = \partial_\mu + ig_{\omega K}\omega_\mu + ig_{\phi K}\phi_\mu + ig_{\rho K}t_K \cdot \boldsymbol{\rho}_\mu$ and the effective mass of (anti)kaons is $m_K^* = m_K - g_{\sigma K}\sigma - g_{\sigma^* K}\sigma^*$. The mixed phase of hadronic and K^- condensed matter is governed by the Gibbs conditions for thermodynamic equilibrium along with global charge and baryon number conservation laws [22]. Working in the mean field approximation, we obtain energy density and pressure in each pure phase and those are given by Ref.[21].

III. RESULTS AND DISCUSSION

Nucleon-meson coupling constants obtained by reproducing saturation properties of nuclear matter for two values of incompressibility $K = 240$ and $K = 300$ MeV, are taken from Ref. [23]. These are known as GM sets. Hyperon-vector meson coupling constants are determined from SU(6) symmetry of the quark model [15, 24, 25]. The scalar meson σ meson coupling to hyperons is calculated from the potential depth of a hyperon (Y)

$$U_Y^N(n_0) = -g_{\sigma Y}\sigma + g_{\omega Y}\omega_0 , \quad (10)$$

in normal nuclear matter. Potential depths of hyperons in normal nuclear matter are obtained from the analysis of hypernuclei data [24, 26, 27, 28]. Similarly hyperon- σ^* coupling constants are estimated by fitting them to a potential depth, $U_Y^{(Y')}(n_0)$, for a hyperon (Y) in hyperon matter. We adopt the values of hyperon potential depths for this calculation as quoted in Ref. [21]. Next we determine kaon-vector meson coupling constants using the quark model and isospin counting rule [17]. The scalar coupling with kaons is obtained from the real part of K^- optical potential depth at normal nuclear matter density [29, 30]

$$U_{\bar{K}}(n_0) = -g_{\sigma K}\sigma - g_{\omega K}\omega_0 , \quad (11)$$

where σ and ω_0 are mean values of the meson fields. We perform our calculation for antikaon condensation with $K = 300$ MeV and two values of antikaon optical potential depth $U_{\bar{K}}(n_0) = -120, -160$ MeV. Values of $g_{\sigma K}$ are recorded in Ref. [21]. Coupling constants $g_{\sigma^* K}$ and $g_{\phi K}$ are obtained from Refs.[15, 21].

Now we present our results for different compositions and equations of state. Gravitational mass for static neutron star as well as superdense star sequences are shown with radius in Figure 1 for different values of incompressibility. For np matter we find the EoS

with $K = 300$ MeV is stiffer than that of the case with $K = 240$ MeV. Consequently the maximum mass is larger in the former case. With the appearance of hyperons and/or antikaon condensates, equations of state become softer. For $np\Lambda$ matter and $K = 300$ MeV, the threshold density of Λ hyperons is $2.3n_0$. On the other hand, for npK^- matter with $K = 300$ MeV, K^- condensation sets in at $2.23n_0$ and the mixed phase terminates at $3.59n_0$ for $U_{\bar{K}}(n_0) = -160$ whereas the phase transition for $U_{\bar{K}}(n_0) = -120$ MeV begins at $3.05n_0$ and there is no mixed phase in this case. Stronger the attractive antikaon optical potential depth, softer is the EoS. Softer EoS involving hyperons and antikaon condensates lead to reduction in maximum masses than that of the np matter as evident from Fig. 1. For $npHK^-\bar{K}^0$ case with $K = 300$ and $U_{\bar{K}}(n_0) = -160$ MeV, Λ hyperons appear at $2.51n_0$ after the onset of K^- condensation at $2.23n_0$. The mixed phase ends at $4.0n_0$ in this case. Further \bar{K}^0 condensation which is treated here as a second order phase transition, begins at $4.06n_0$ [21]. Heavier strange baryons are populated beyond $6n_0$ [21]. For $npHK^-\bar{K}^0$ case, it was noted that after the stable neutron star branch, there was an unstable region followed by another stable branch of compact stars [21]. As white dwarfs and neutron stars form first two families of compact stars, this branch of superdense stars beyond the neutron star branch is called the third family of compact stars [31]. Further the existence of non-identical stars having same mass could be possible because of partial overlapping of the neutron star and third family branches. These pairs of compact stars are known as "neutron star twins" [32, 33]. Superdense stars in the third family branch have different compositions and smaller radii than their counterparts in the neutron star branch [21].

Next we calculate the frequency (ν) and damping time (τ) from Eq. (2) using equations of state described above. We exploit both the continued fraction method [10] and integration method [7] to find complex eigenfrequency of the Schrödinger like equation (2). Here we present our results obtained by using the continued fraction method. The frequency and damping time are related to the real and imaginary parts of eigenfrequency through $\nu = \frac{32.26}{n}(M\omega_0)$ kHz and $\tau = 4.937 \times \frac{n}{M\omega_i}$ μ s, where $n=M/M_\odot$ and ω_0, ω_i, M and M_\odot are measured in units of km. Figures 2 and 3 display frequency and damping time of first axial w-mode as a function of neutron star compactness (M/R) respectively. In both figures, the dashed line corresponds to np matter with $K = 240$ MeV whereas the solid line represents np case with $K = 300$ MeV. We note that the softer EoS leads to higher frequency of first axial w-mode for each M/R value as shown in Fig. 2 whereas it is the reverse for damping

time as evident from Fig. 3.

In the next paragraphs we discuss the role of exotic matter on frequency and damping time of axial w-mode. Firstly we study axial w-modes of neutron stars involving $np\Lambda$ matter along with those of np matter for $K = 300$ MeV. Frequencies and damping times of first axial w-mode for both cases are exhibited in Figures 4 and 5. The appearance of Λ hyperons makes the EoS softer compared with the np case. This leads to higher frequencies of first axial modes for oscillating neutron stars including Λ hyperons as shown by the upper curve in Fig. 4 whereas damping times in this case are given by the lower curve in Fig. 5. Frequencies and damping times of first three $l = 2$ axial w-modes corresponding to the EoS involving $np\Lambda$ matter with increasing compactness are recorded in Table I.

We continue our investigation of first axial w-modes of neutron stars including a first order K^- condensate. These results are shown in Figures 6 and 7. We have considered two values of antikaon optical potential depth at normal nuclear matter density $U_{\bar{K}} = -120, -160$ MeV. For $U_{\bar{K}} = -160$ MeV, frequencies of first axial w-modes for neutron stars having a K^- condensate are shown by the top curve whereas those of npK^- EoS for $U_{\bar{K}}(n_0) = -120$ MeV have lower frequencies. This may be attributed to the fact that the EoS with $U_{\bar{K}}(n_0) = -160$ is softer than that of $U_{\bar{K}}(n_0) = -120$ MeV. Similarly we find that damping times for $U_{\bar{K}}(n_0) = -160$ MeV are reduced than those of $U_{\bar{K}}(n_0) = -120$ MeV and np case. Frequencies and damping times of first three $l = 2$ axial w-modes of oscillating neutron stars including a K^- condensate with increasing compactness are recorded in Table II.

Frequencies and damping times of first axial w-modes of neutron star as well as third family sequences as a function of compactness are shown in Figures 8 and 9. In Fig. 8 frequencies of first axial w-modes corresponding to the neutron star and third family branches are denoted by the bottom and top curves respectively. Further twins of superdense stars in the third family branch (top curve) are represented by filled squares in the neutron star branch (bottom curve). Keeping baryon number fixed, the collapse of an ordinary neutron star to its twin in the third family branch might release huge amount of energy. A part of it may be carried away by gravitational waves. This could be a good signal to probe interior of superdense stars. Damping times of superdense stars corresponding to the third family branch have higher values than those of the neutron star branch.

We compare real and imaginary parts of eigenfrequencies of first axial w-modes for EoS including $np\Lambda$ and EoS involving npK^- with $U_{\bar{K}}(n_0) = -160$ MeV in Figures 10 and 11.

We find that values of real and imaginary frequencies corresponding to both EoS are close beyond compactness 0.18. We conclude from these results and those recorded in Table I and II that these equations of state are indistinguishable in axial w-modes.

IV. SUMMARY AND CONCLUSIONS

We have studied quasi-normal modes of oscillating neutron stars with different compositions and equations of state. This problem has been investigated adopting continued fraction method. We have computed frequencies and damping time scales of axial w-modes corresponding to EoS involving np , $np\Lambda$ and npK^- and $npHK^-\bar{K}^0$ matter. We find that hyperons and/or antikaon condensates result softer EoS which, in turn, lead to higher frequencies and lower damping time compared with those of np case. Axial w-modes might distinguish between exotic matter and nucleons-only matter. However, it would be difficult to differentiate the EoS of hyperon matter from that of antikaon condensed matter using axial w-modes as probe. Further our study has revealed that frequencies of superdense stars in third family branch are higher than their twins in the neutron star branch.

-
- [1] N.K. Glendenning, Compact stars, (Springer, New York, 1997).
 - [2] B. J. Owen, arXiv:**0903.2603**[astro-ph]
 - [3] N. Andersson and K.D. Kokkotas, Mon. Not. R. Astron. Soc. **299**, 1059 (1998).
 - [4] N. Andersson and K.D. Kokkotas, Int. J. Mod. Phys. **D10**, 381 (2001).
 - [5] S. Chandrasekhar and V. Ferrari, Proc. R. Soc. Lond. **A432**, 247 (1991).
 - [6] S. Chandrasekhar and V. Ferrari, Proc. R. Soc. Lond. **A434**, 449 (1991).
 - [7] K.D. Kokkotas, Mon. Not. R. Astron. Soc. **268**, 1015 (1994).
 - [8] M. Leins, H. -P. Nollert and M. H. Soffel, Phys. Rev. **D48**, 3467 (1993).
 - [9] V. Ferrari and L. Gualtieri, Gen. Rel. Grav. 40 (2008) 945
 - [10] O. Benhar, E. Berti and V. Ferrari, Mon. Not. R. Astron. Soc. **310**, 797 (1999).
 - [11] O. Benhar, Mod. Phys. Lett. **A20**, 2335 (2005).
 - [12] L.K. Tsui, P.T. Leung and J. Wu, Phys. Rev. **D74**, 124025 (2006).
 - [13] D.B. Kaplan and A.E. Nelson, Phys. Lett. B **175**, 57 (1986);

- A.E. Nelson and D.B. Kaplan, Phys. Lett. B **192**, 193 (1987).
- [14] E. Farhi and R. L. Jaffe, Phys. Rev. **D30**, 2379 (1984).
- [15] J. Schaffner and I.N. Mishustin, Phys. Rev. C **53**, 1416 (1996).
- [16] J. Boguta and A. R. Bodmer, Nucl. Phys. **A292**, 413 (1977).
- [17] N.K. Glendenning and J. Schaffner-Bielich, Phys. Rev. Lett. **81**, 4564 (1998).
- [18] N.K. Glendenning and J. Schaffner-Bielich, Phys. Rev. **C60**, 025803 (1999).
- [19] S. Pal, D. Bandyopadhyay and W. Greiner, Nucl. Phys. **A674** (2000) 553
- [20] S. Banik and D. Bandyopadhyay, Phys. Rev. **C63**, 035802 (2001).
- [21] S. Banik and D. Bandyopadhyay, Phys. Rev. **C64**, 055805 (2001).
- [22] N.K. Glendenning, Phys. Rev. **D46**, 1274 (1992).
- [23] N.K. Glendenning and S.A. Moszkowski, Phys. Rev. Lett. **67**, 2414 (1991).
- [24] C. B. Dover and A. Gal, Prog. Part. Nucl. Phys. **12**, 171 (1984).
- [25] J. Schaffner, C.B. Dover, A. Gal, D. J. Millener, C. Greiner and H. Stöcker, Ann. Phys. (N.Y.) **235**, 35 (1994).
- [26] R. E. Chrien and C. B. Dover, Annu. Rev. Nucl. Part. Sci. **39**, 113 (1989).
- [27] T. Fukuda et al., Phys. Rev. C **58**, 1306 (1998).
- [28] P. Khaustov et al., Phys. Rev. C **61**, 054603 (2000).
- [29] E. Friedman, A. Gal and C.J. Batty, Nucl. Phys. **A579**, 518 (1994);
C.J. Batty, E. Friedman and A. Gal, Phys. Rep. **287**, 385 (1997).
- [30] E. Friedman, A. Gal, J. Mareš and A. Cieplý, Phys. Rev. C **60**, 024314 (1999).
- [31] U. H. Gerlach, Phys. Rev. **172**, 1325 (1968).
- [32] N.K. Glendenning and C. Kettner, Astron. Astrophys. **353**, L9 (2000).
- [33] K.Schertler, C. Greiner, J. Schaffner-Bielich and M. H. Thoma, Nucl. Phys. **A677**, 463 (2000).

TABLE I: First three values of characteristic $l=2$ axial w -mode frequencies and damping timescales for neutron stars made of n , p , Λ and electrons and muons.

M	R	$\frac{M}{R}$	ν	τ
(M_{\odot})	(km)		(kHz)	(μs)
1.822	12.892	0.2	6.830	79.571
			10.055	47.711
			13.391	50.397
1.867	12.325	0.22	6.796	87.129
			9.8556	52.440
			12.800	51.996
1.885	11.514	0.24	6.800	94.766
			9.595	60.417
			12.148	54.029

TABLE II: The first three values of characteristic $l=2$ axial w -mode frequencies and damping timescales for neutron stars undergoing a first order phase transition from nuclear to K^- condensed matter for antikaon optical potential depth at normal nuclear matter density $U_{\bar{K}}(n_0) = -160\text{MeV}$.

M	R	$\frac{M}{R}$	ν	τ
(M_\odot)	(km)		(kHz)	(μs)
1.680	12.401	0.2	6.996	69.554
			10.107	46.401
			13.691	51.040
1.770	11.641	0.22	6.941	80.302
			9.832	52.712
			12.779	53.119
1.825	11.068	0.24	6.900	89.476
			9.593	60.270
			12.149	54.333

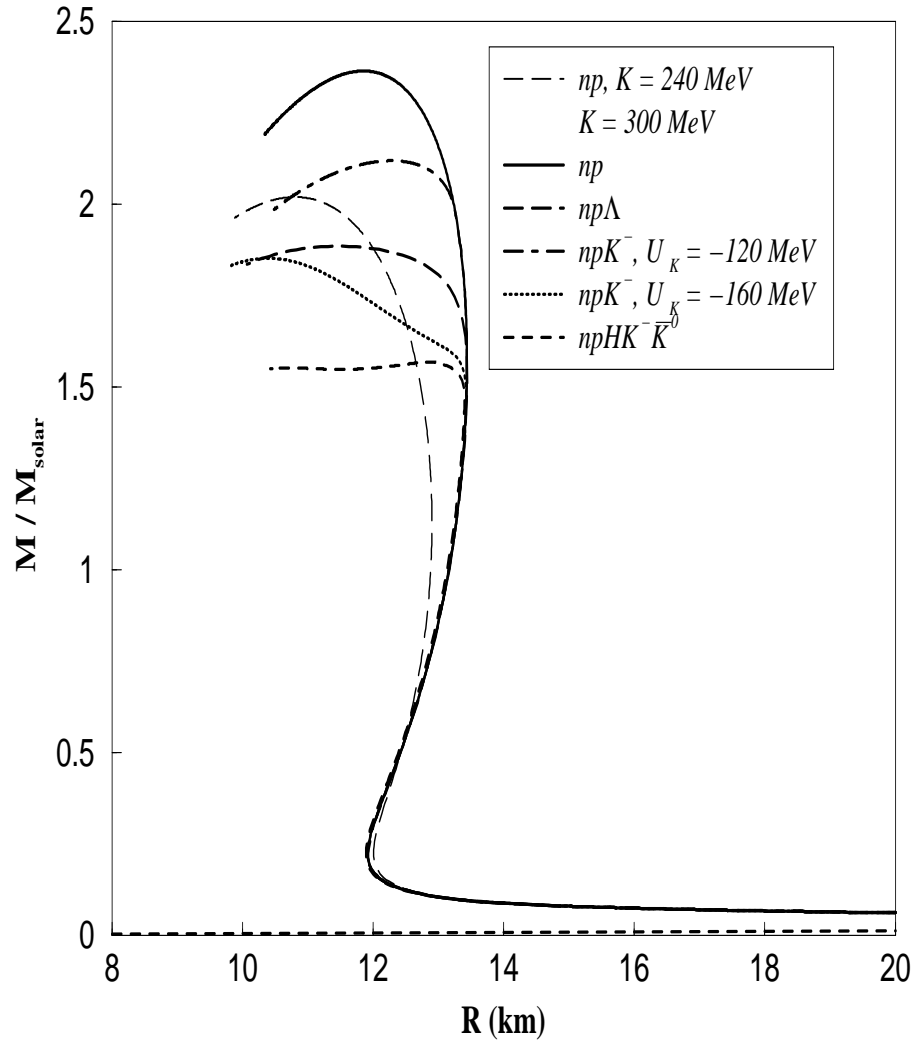


Fig. 1. Gravitational mass is plotted with radius for compact stars having different compositions as explained in text.

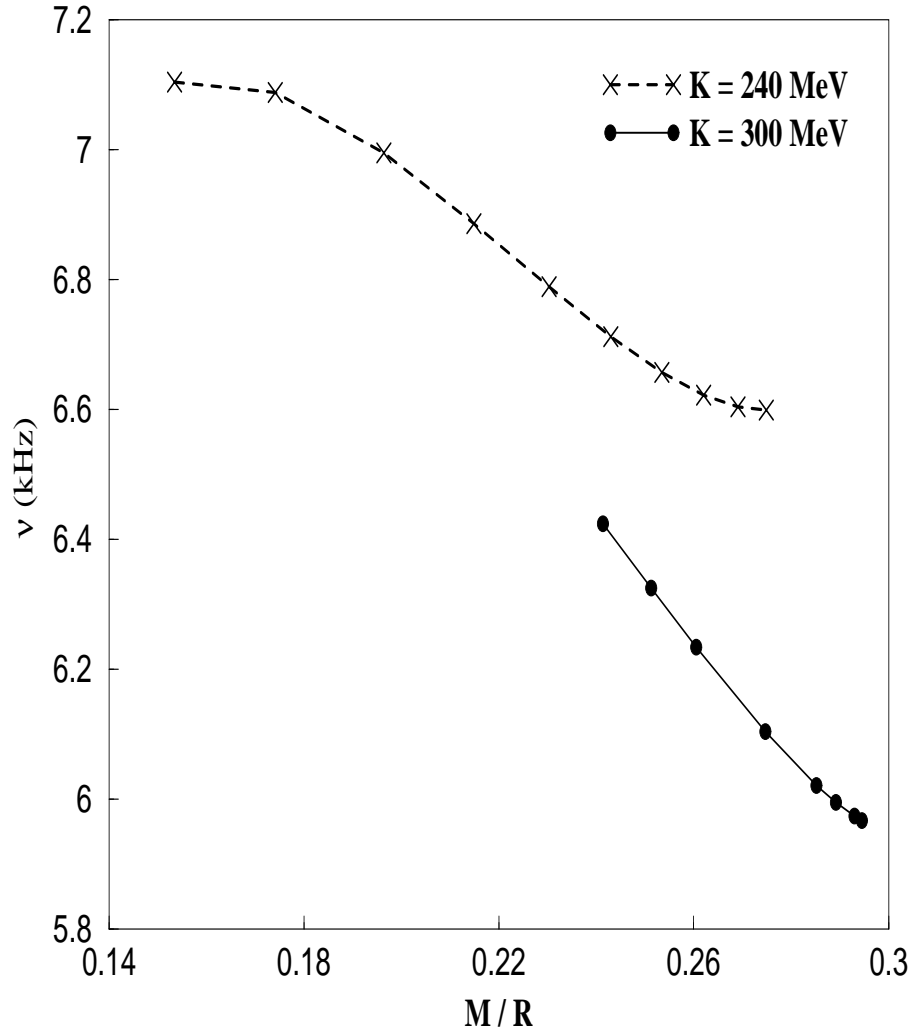


Fig. 2. Frequency of first axial w-mode is plotted as a function of neutron star compactness for nucleons only matter corresponding to incompressibility $K=240$ and 300 MeV.

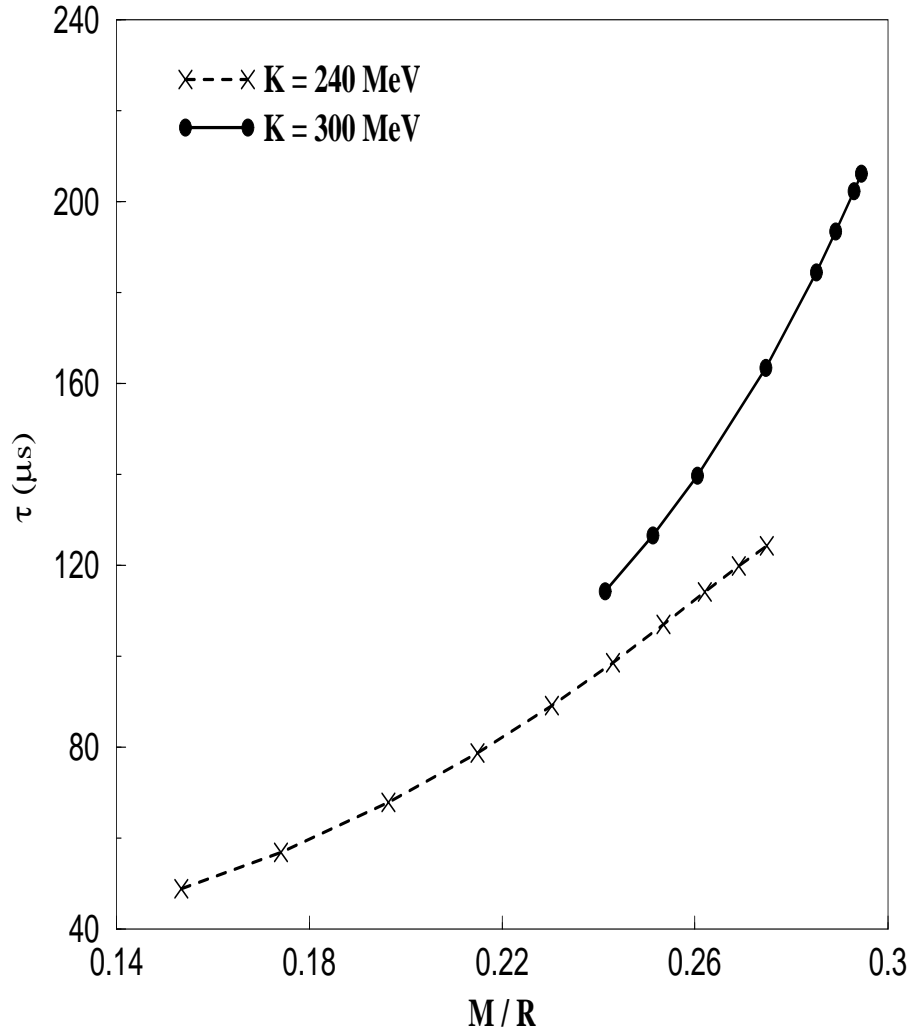


Fig. 3. Damping time of first axial w-mode is plotted as a function of neutron star compactness for nucleons only matter corresponding to incompressibility $K=240$ and 300 MeV.

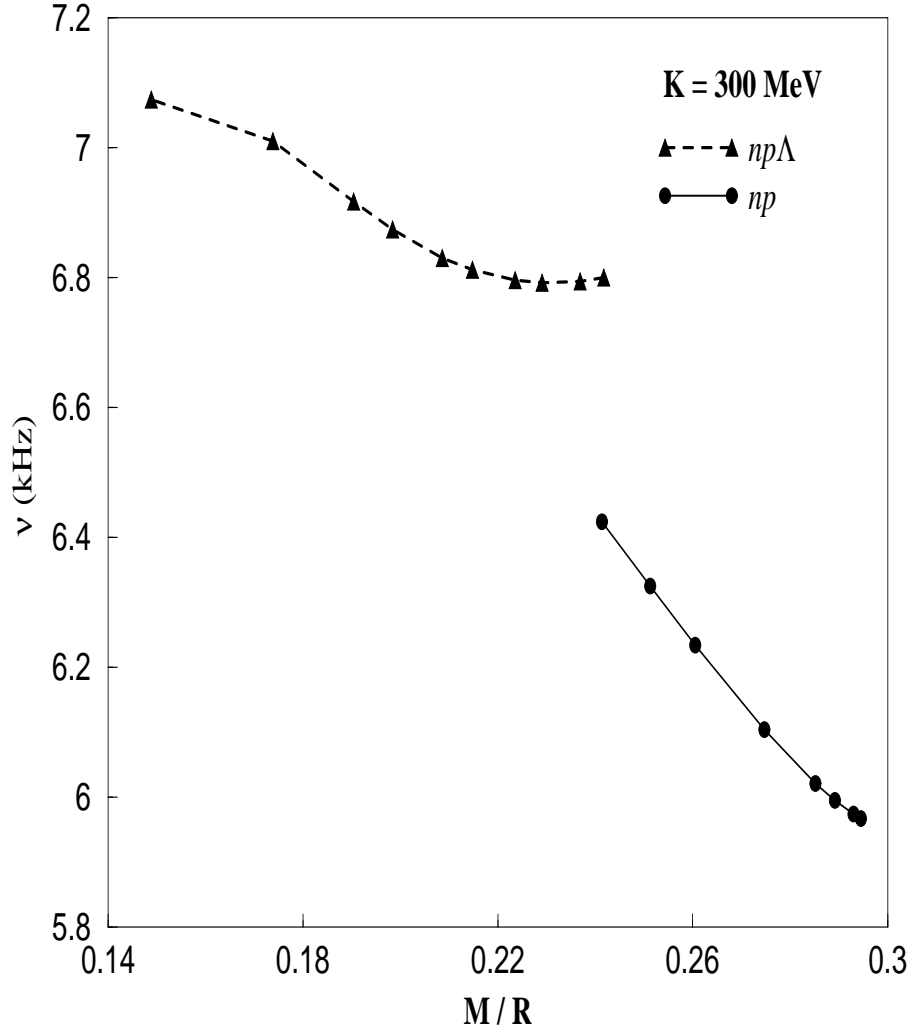


Fig. 4. Frequency of first axial w-mode is plotted as a function of neutron star compactness for *np* as well as *np*Λ matter with $K=300$ MeV.

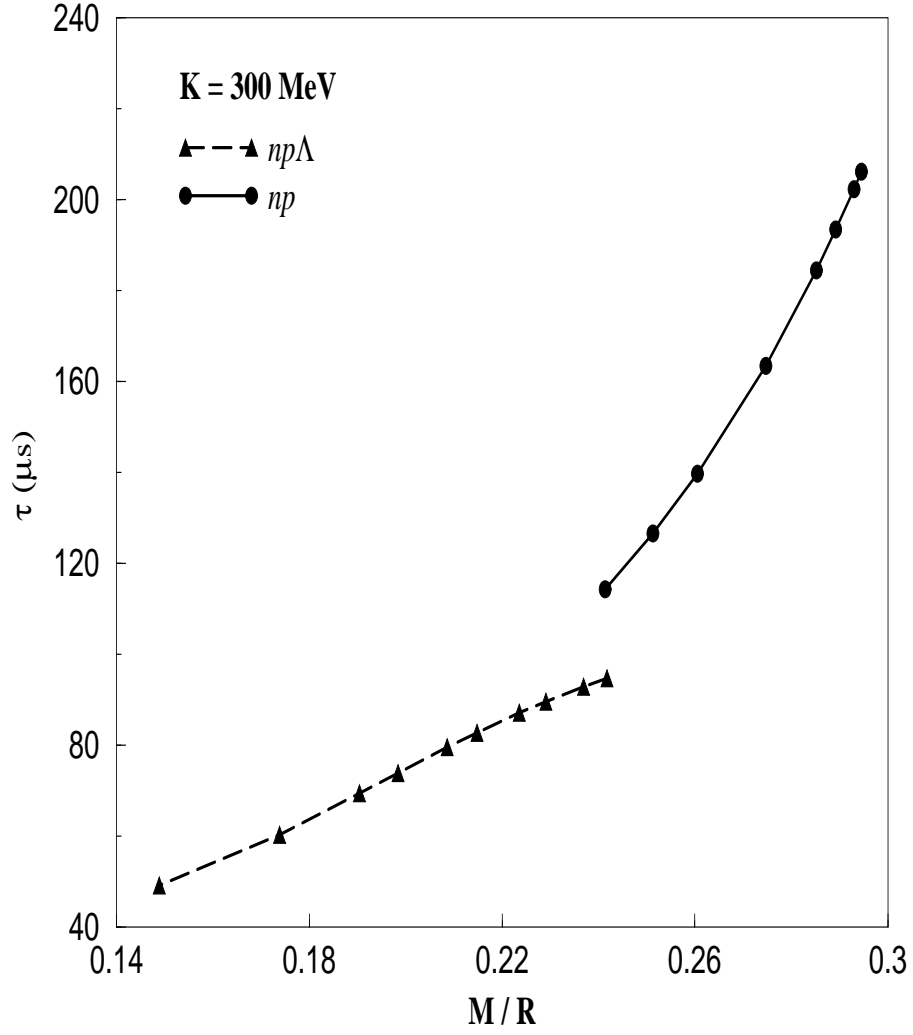


Fig. 5. Damping time of first axial w-mode is plotted as a function of neutron star compactness for np as well as $np\Lambda$ matter with $K=300$ MeV.

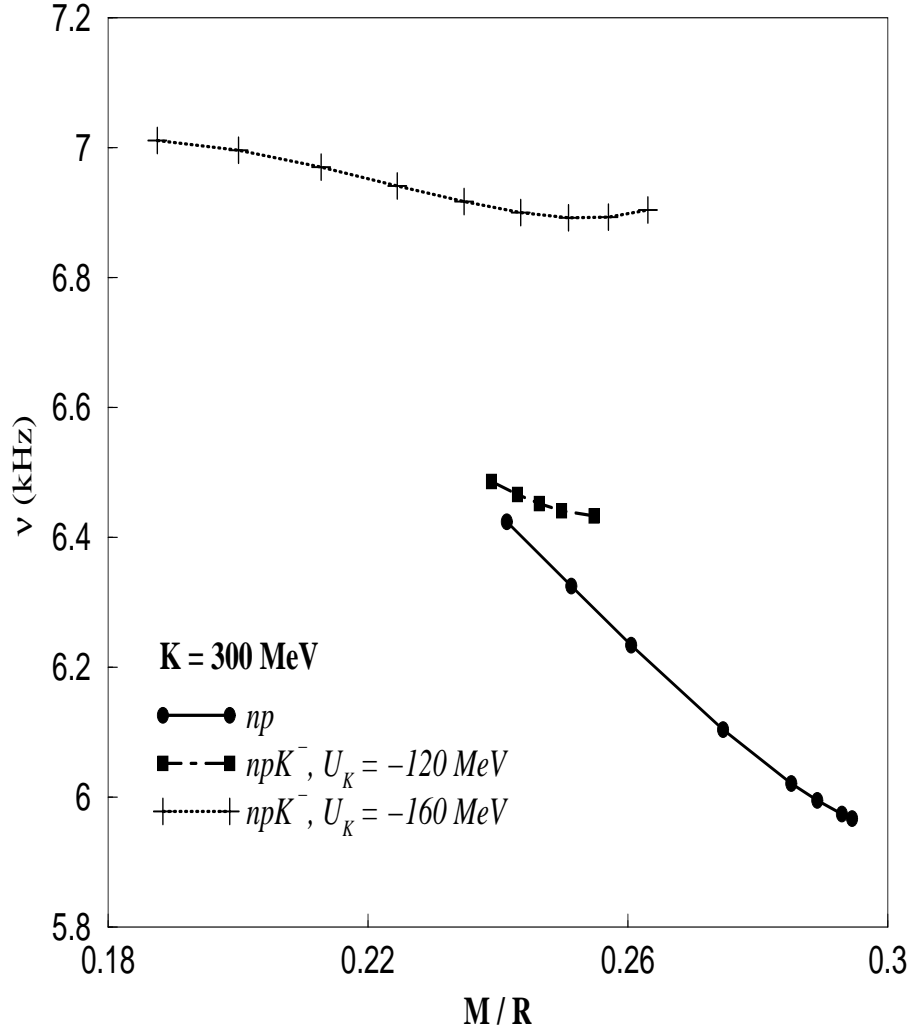


Fig. 6. Frequency of first axial w-mode is plotted as a function of neutron star compactness for np and npK^- matter with $K=300 \text{ MeV}$ and $U_{\bar{K}}(n_0) = -120, -160 \text{ MeV}$.

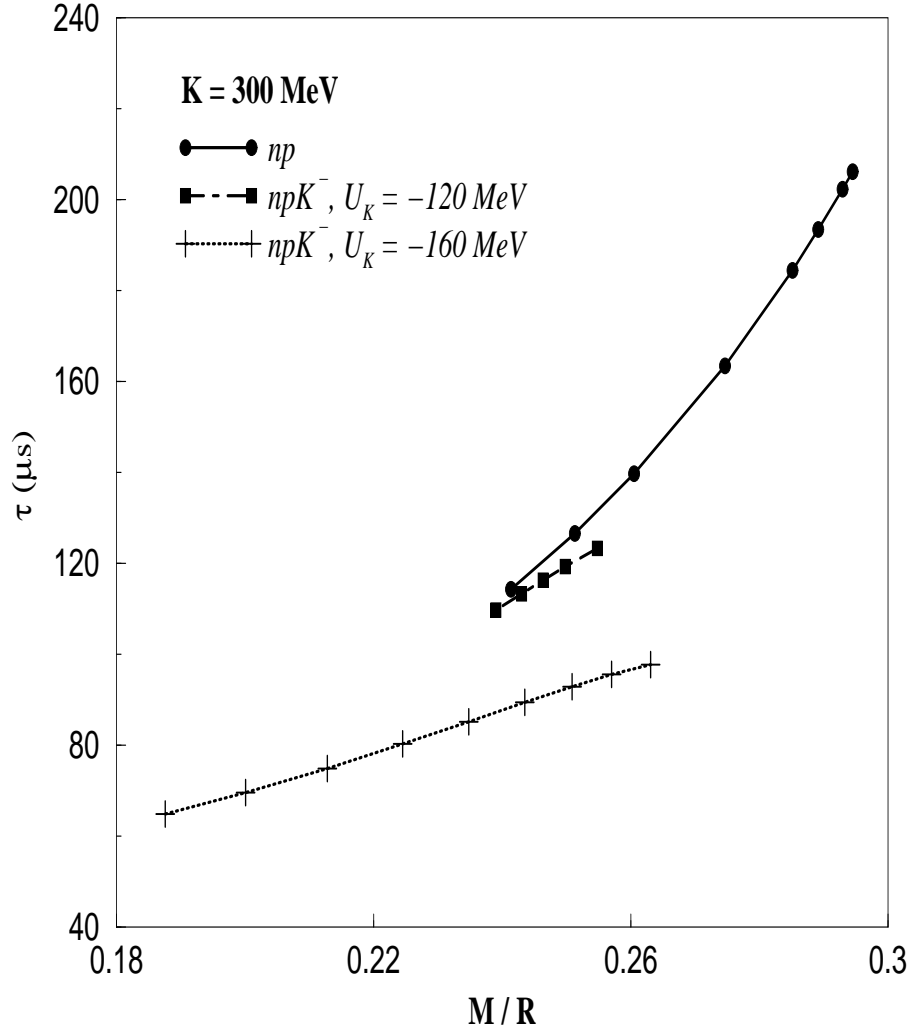


Fig. 7. Damping time of first axial w -mode is plotted as a function of neutron star compactness for np and npK^- matter with $K=300 \text{ MeV}$ and $U_{\bar{K}}(n_0) = -120, -160 \text{ MeV}$.

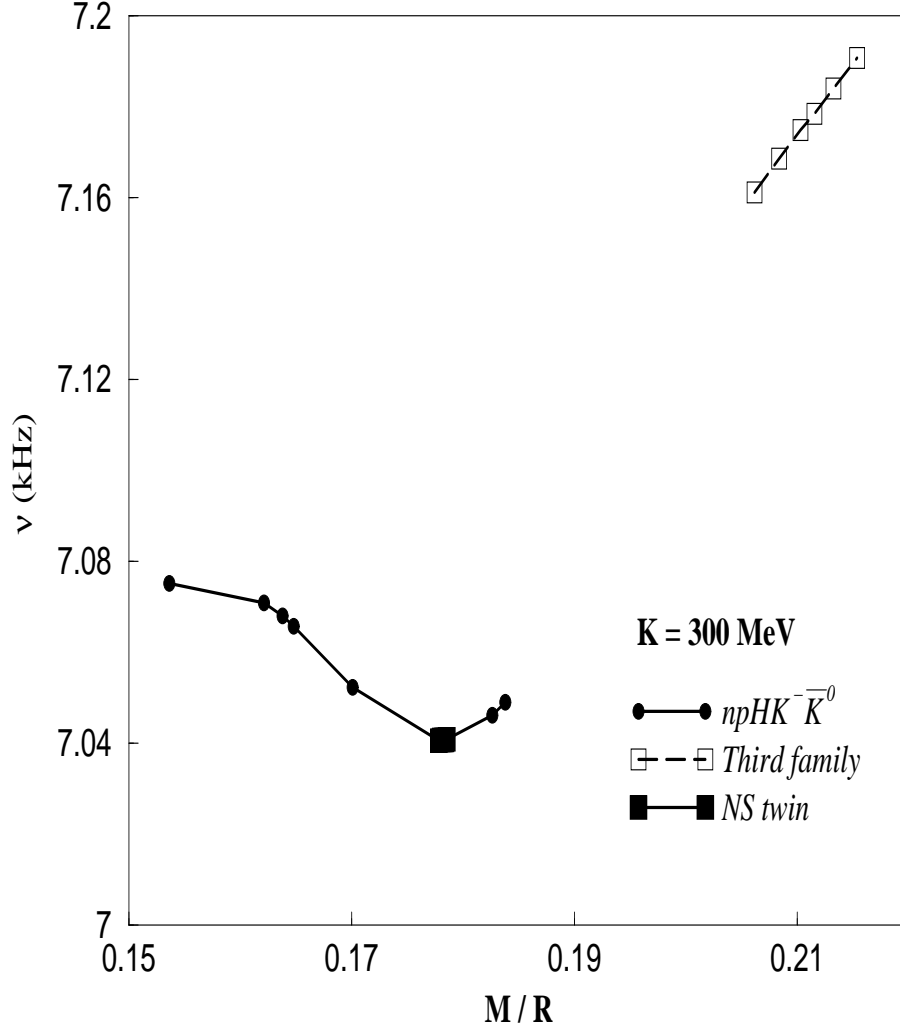


Fig. 8. Frequency of first axial w-mode is plotted as a function of compactness for neutron stars including $n, p, \Lambda, \Xi^-, \Xi^0, \Sigma^-, K^-$ and \bar{K}^0 with $K=300$ MeV and $U_{\bar{K}}(n_0) = -160$ MeV. The lower curve shows the neutron star branch whereas the third family branch is shown by the upper curve. Neutron star twins corresponding to the superdense stars in the third family branch are denoted by filled squares in the lower curve.

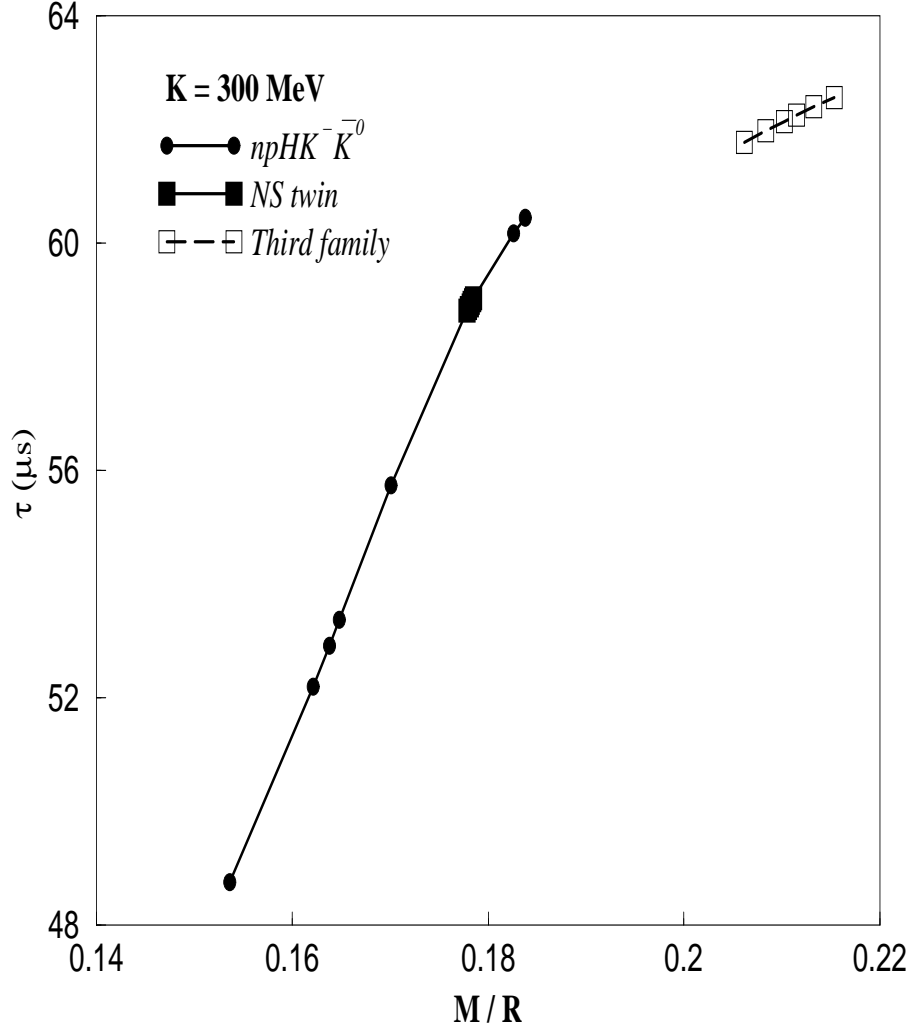


Fig. 9. Damping time of first axial w-mode is plotted as a function of compactness for neutron stars including $n, p, \Lambda, \Xi^-, \Xi^0, \Sigma^-, K^-, \bar{K}^0$ with $K=300$ MeV and $U_{\bar{K}}(n_0) = -160$ MeV. The lower curve shows the neutron star branch whereas the third family branch is shown by the upper curve. Neutron star twins corresponding to the superdense stars in the third family branch are denoted by filled squares in the lower curve.

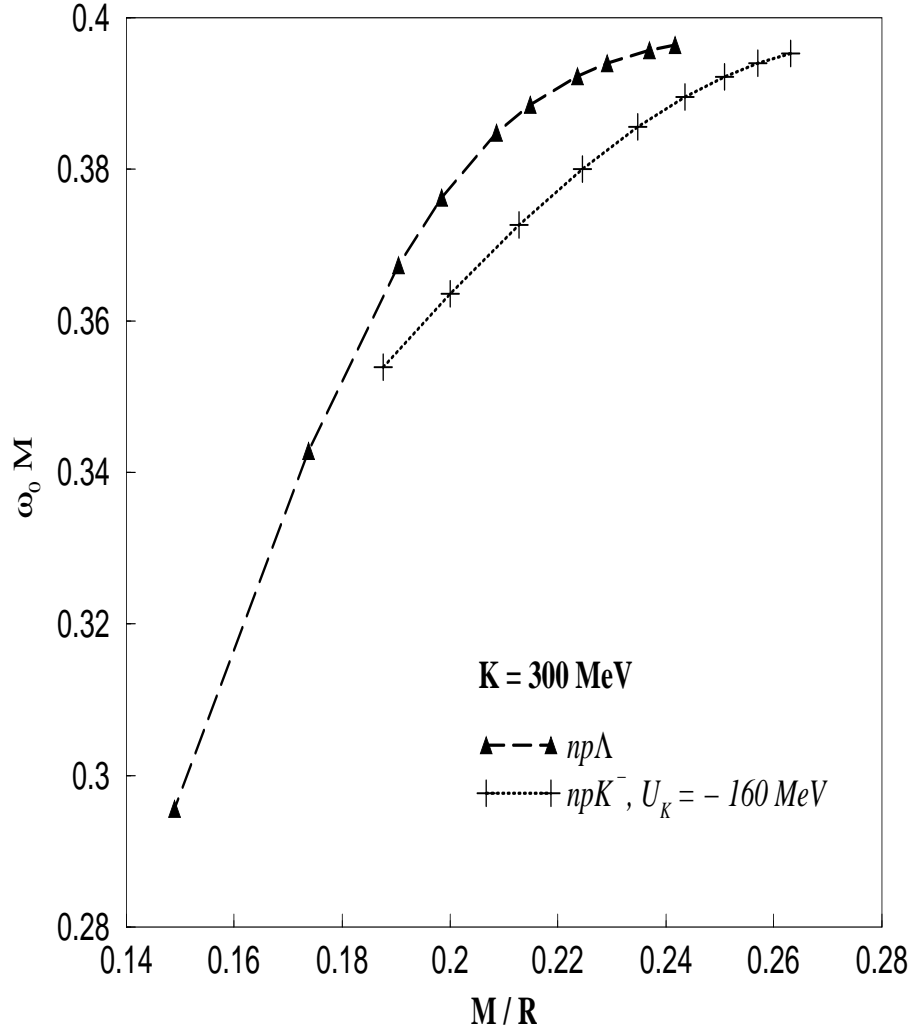


Fig. 10. Real part of eigenfrequency of first axial w-mode is plotted as a function of compactness for $np\Lambda$ and npK^- matter with $K=300$ MeV and $U_{\bar{K}}(n_0) = -160$ MeV.

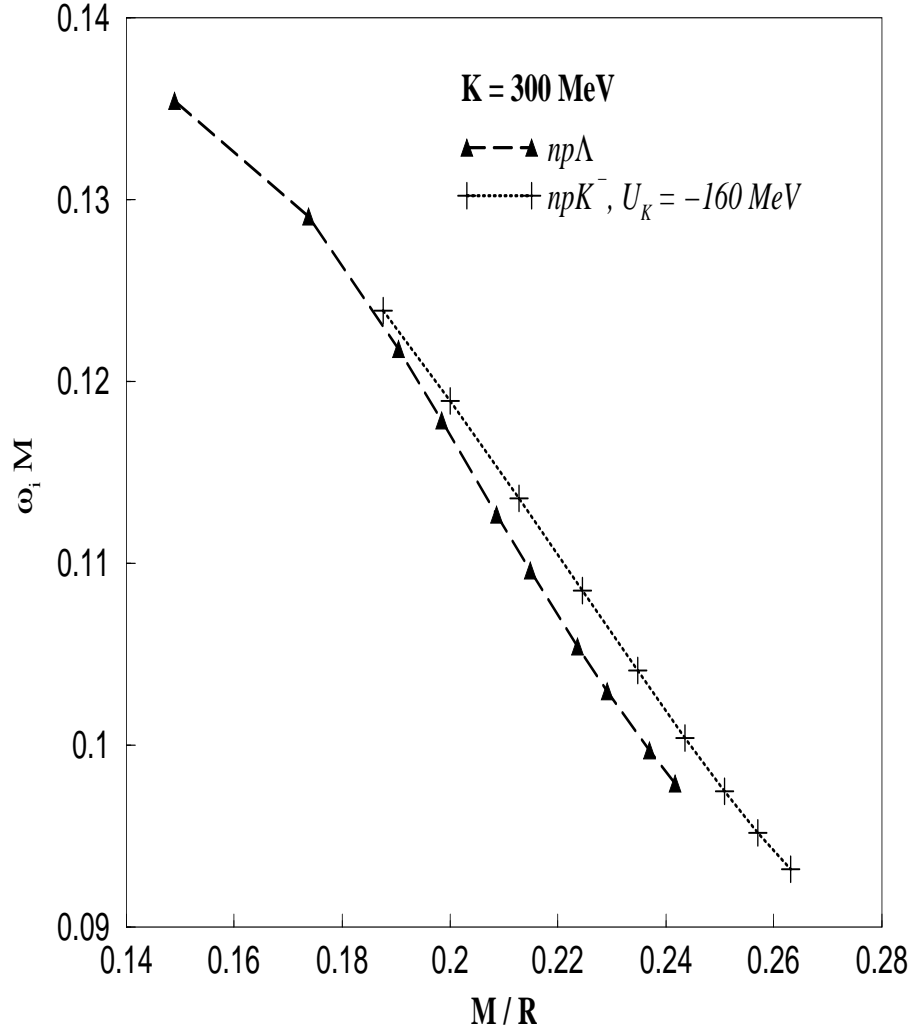


Fig. 11. Imaginary part of eigenfrequency of first axial w-mode is plotted as a function of compactness for $np\Lambda$ and npK^- matter with $K=300 \text{ MeV}$ and $U_{\bar{K}}(n_0) = -160 \text{ MeV}$.